

Review Article

Open Access



# Recent advancements in liquid metal enabled flexible and wearable biosensors

Guoqiang Li<sup>1,#</sup>, Sanhu Liu<sup>2,#</sup>, Zhiwu Xu<sup>2</sup>, Jinhong Guo<sup>3,\*</sup>, Shi-Yang Tang<sup>4,5,\*</sup> , Xing Ma<sup>1,2,\*</sup>

<sup>1</sup>Sauvage Laboratory for Smart Materials, School of Materials Science and Engineering, Harbin Institute of Technology (Shenzhen), Shenzhen 518055, Guangdong, China.

<sup>2</sup>State Key Laboratory of Advanced Welding and Joining, Harbin Institute of Technology, Harbin 150001, Heilongjiang, China.

<sup>3</sup>School of Sensing Science and Engineering, Shanghai Jiaotong University, Shanghai 200240, China.

<sup>4</sup>Department of Electronic Electrical and Systems Engineering, University of Birmingham, Edgbaston, Birmingham B15 2TT, UK.

<sup>5</sup>School of Electronics and Computer Science, University of Southampton, Southampton SO17 1BJ, UK.

#Authors contributed equally.

\*Correspondence to: Prof. Xing Ma, Sauvage Laboratory for Smart Materials, School of Materials Science and Engineering, Harbin Institute of Technology (Shenzhen), No. 6 Pingshan 1st Road, Shenzhen 518055, Guangdong, China. E-mail: maxing@hit.edu.cn; Prof. Shi-Yang Tang, Department of Electronic Electrical and Systems Engineering, University of Birmingham, Edgbaston Park Rd, Edgbaston, Birmingham B15 2TT, UK. E-mail: Shiyang.Tang@soton.ac.uk; Prof. Jinhong Guo, School of Sensing Science and Engineering, Shanghai Jiao Tong University, 1954 Huashan Road, Xuhui District, Shanghai 200240, China. E-mail: guojinhong@sjtu.edu.cn

**How to cite this article:** Li G, Liu S, Xu Z, Guo J, Tang SY, Ma X. Recent advancements in liquid metal enabled flexible and wearable biosensors. *Soft Sci* 2023;3:37. <https://dx.doi.org/10.20517/ss.2023.30>

**Received:** 28 Jun 2023 **First Decision:** 28 Jul 2023 **Revised:** 13 Aug 2023 **Accepted:** 22 Aug 2023 **Published:** 16 Oct 2023

**Academic Editor:** Zhifeng Ren **Copy Editor:** Pei-Yun Wang **Production Editor:** Pei-Yun Wang

## Abstract

Wearable biosensors have demonstrated enormous potential in revolutionizing healthcare by providing real-time fitness tracking, enabling remote patient monitoring, and facilitating early detection of health issues. To better sense vital life signals, researchers are increasingly favoring wearable biosensors with flexible properties that can be seamlessly integrated with human tissues, achieved through the utilization of soft materials. Gallium (Ga)-based liquid metals (LMs) possess desirable properties, such as fluidity, high conductivity, and negligible toxicity, which make them inherently soft and well-suited for the fabrication of flexible and wearable biosensors. In this article, we present a comprehensive overview of the recent advancements in the nascent realm of flexible and wearable biosensors employing LMs as key components. This paper provides a detailed exposition of the unique characteristics of Ga-based LM materials, which set them apart from traditional materials. Moreover, the state-of-the-art applications of Ga-based LMs in flexible and wearable biosensors that expounded from six aspects are reviewed, including wearable interconnects, pressure sensors, strain sensors, temperature sensors, and implantable bioelectrodes. Furthermore, perspectives on the key challenges and future developing directions of



© The Author(s) 2023. **Open Access** This article is licensed under a Creative Commons Attribution 4.0 International License (<https://creativecommons.org/licenses/by/4.0/>), which permits unrestricted use, sharing, adaptation, distribution and reproduction in any medium or format, for any purpose, even commercially, as long as you give appropriate credit to the original author(s) and the source, provide a link to the Creative Commons license, and indicate if changes were made.



LM-enabled wearable and flexible biosensors are also discussed.

**Keywords:** Liquid metal, flexible electronics, biosensors, wearable electronics

## INTRODUCTION

Wearable biosensors are directly worn inside or outside the body in the form of watches, bracelets, glasses, and clothing to acquire real-time and useful information related to heart rate<sup>[1-3]</sup>, blood oxygen<sup>[4,5]</sup>, exercise<sup>[6-8]</sup>, and other physiological signals<sup>[9-11]</sup>. The key consideration for wearable biosensors is the comfort of individuals who wear the devices during routine activities without restricting sensing precision<sup>[12]</sup>. Conventionally, wearable biosensors have been fabricated from rigid materials, limiting their comfort during use and compromising safety for implantation. Thus, the development of biosensors with flexible and stretchable properties is crucial to allow for conformal integration onto human skin and tissue, facilitating optimal signal acquisition and transmission.

In recent years, gallium (Ga)-based liquid metals (LMs) have transcended their role in many fields, finding diverse applications across multiple disciplines. From soft robotics and advanced electronics to additive manufacturing and biomedicine, their exceptional properties have fostered innovation and paved the way for transformative breakthroughs in various fields<sup>[13-15]</sup>. Especially in the field of flexible and wearable electronics, attributed to their unique mechanical/chemical properties, Ga-based LMs have attracted much attention. These properties include (1) LMs are in a liquid state with good fluidity at room temperature, resulting in negligible Young's modulus that can avoid the mechanical interface mismatch between the device and human tissue<sup>[15-17]</sup>; (2) they are metallic materials with high electrical/thermal conductivity, which are essential for conducting electricity and heat transfer of wearable biosensors<sup>[18,19]</sup>; and (3) the low toxicity of LMs satisfies the bio-friendly requirements of wearable electronics<sup>[20,21]</sup>. In addition, patterning technologies depending on the native physical properties of LMs, such as channel injection<sup>[22,23]</sup>, direct writing<sup>[24-26]</sup>, and spray-printing<sup>[27]</sup> methods, have greatly enabled the fabrication of LM-based wearable and flexible sensors. Various wearable biosensors that are mountable on human tissue have been developed using LMs. These biosensors have expanded the scope of wearable electronics and can be utilized in numerous areas, such as human-machine interface, motion detection, and health monitoring.

This review aims to summarize the basic physical properties of LM-based materials and provides an in-depth introduction to the designs/applications of flexible/stretchable interconnects, pressure sensors, strain sensors, and implantable electrodes based on LMs [Figure 1]. This review begins with providing a detailed description of the physical properties and electrically conductive mechanisms of LMs-based materials, including raw LMs, LM nanoparticles (LMNPs) inks, and LM-polymer composites. The second section summarizes recent advancements in LM-based biosensing devices, including interconnections, pressure sensors, strain sensors, and implantable bioelectrodes. These advancements include nano-scale LM circuits for improved bioelectronic integration, enhanced sensitivity of LM pressure sensors for monitoring gastrointestinal pressure, fiber-featured strain sensors for breathing monitoring, and implantable bioelectrodes capable of sensing electroencephalogram (EEG)/electrocardio (ECG) signals. These recently developed LM-based biosensors offer exciting opportunities for *in vivo/vitro* monitoring of heart rate, breath rate, body movement, and EEG/ECG signals. At last, the final section discusses the challenges and future research perspectives of LM-based biosensors.

## GA-BASED LMS, LMNP INKS, AND LM-ELASTOMER COMPOSITES

### Raw LMs

Ga and Ga-based alloys are the most popular used LMs for flexible electronics when compared to liquid-

state metals, such as mercury (Hg), rubidium (Rb), cesium (Cs), and francium (Fr). This is due to their unique physical properties, such as relatively stable chemical properties in air and water, low melting point<sup>[15]</sup>, high electrical/thermal conductivities<sup>[28,29]</sup>, low viscosity<sup>[28,29]</sup>, and low toxicity<sup>[30]</sup>. Pure Ga alloys with a melting point of 29.8 °C are solid-state at room temperature. The addition of In and Sn alloys through alloying can reduce the melting point (e.g., the melting point of Galinstan with 20.5 wt.% In and 12.5 wt.% Sn is 11 °C). One important characteristic of Ga-based LMs is their low crystallization temperature, which is significantly lower than their melting point. This phenomenon is known as the supercooling effect<sup>[31,32]</sup>. The supercooling effect enables Ga-based LMs to remain in a liquid state at temperatures far below their melting point, thereby expanding the working temperature range for LM-based flexible and wearable electronics. This feature is critical for ensuring the working stability of these devices. In addition, viscosity is one of the essential parameters for patterning bulk LM into specific 2D/3D structures. The viscosity of Ga-based LMs is comparably low, approximately twice that of water<sup>[33]</sup>. The viscosity of LMs can be adjusted through the alloying process. For instance, the viscosity of eutectic Ga-In (EGaIn) is  $1.99 \times 10^{-3}$  kg/m/s, which is lower than pure liquid Ga ( $2.04 \times 10^{-3}$  kg/m/s).

**Toxicity:** Unlike mercury, Ga-based LMs can remain stable at room temperature, attributed to their negligible vapor pressure and solubility in water<sup>[19]</sup>. Although the toxicity of LMs remains controversial, more recent reports suggest that LMs are relatively safe for biological applications. Chitambar and White *et al.* have summarized the medical applications, toxicities, and health impacts of Ga and its compounds<sup>[34,35]</sup>. Ga-based LMs are relatively safe to be applied to medical treatment. For example, LM-printed electronics applied to the skin for tumor-treating field therapy exhibit no obvious side effects<sup>[36]</sup>. EGaIn/calcium alginate hydrogel can be used as a candidate for endovascular embolization and tumor embolotherapy with low toxicity<sup>[37]</sup>. Furthermore, Ga-based LM electrodes showed no adverse effects on the growth of neurons within the culture platform and were able to effectively simulate target neurons<sup>[38]</sup>. The mechanism of the low toxicity of LMs remains elusive, and it might relate to the following factors. On the one hand, Ga-based LMs can be degraded in body fluid, and the metabolites of LMs can be excreted to the outside of the body in the manner of both fecal and renal excretions<sup>[39]</sup>. On the other hand, for wearable flexible electronics, LMs are ordinarily encapsulated within biocompatible elastomers. Indirect contact between LMs and tissue further ensures the safety of biological applications. However, studies about the toxicity of LMs are unsystematic, and more rigorous research should be applied to understand the influence of LMs on human health. Nevertheless, it is essential to continue studying the toxicity of Ga-based LMs and to exercise caution during their fabrication and application processes<sup>[15,40]</sup>.

**Oxidation and Wettability:** Similar to other metals such as aluminum, magnesium, and copper alloys, a self-limiting growth  $\text{Ga}_2\text{O}_3$  oxide layer immediately forms on the surface of LMs when the oxygen concentration is higher than the ppm level<sup>[41]</sup>. The thickness of the oxide layer is associated with the oxygen concentration ( $\sim 0.7$  nm under vacuum conditions and much thicker at ambient conditions)<sup>[42-44]</sup>. It is elastic and stable under critical yield surface stress ( $\sim 0.5$ - $0.6$  N/m). Only when the stress is above the yield strength, the oxide layer will rupture and the fresh LM flows out<sup>[44]</sup>. Attributed to the oxide layer, the wettability and surface tension of LM droplets are significantly altered. Furthermore, oxidizing LMs is an important method to control the wettability for patterning circuits on different substrates<sup>[45-47]</sup>.

### LMNP ink

Although Ga-based LMs possess tremendous advantages for the fabrication of flexible and wearable biosensors, the ability to fabricate biosensors using high-efficiency preparation methods remains constrained by their high surface tension<sup>[44,47]</sup>. Besides, directly using raw LMs as the patterning material leads to high resource consumption, which will increase the costs and limit their market competitiveness<sup>[48]</sup>.

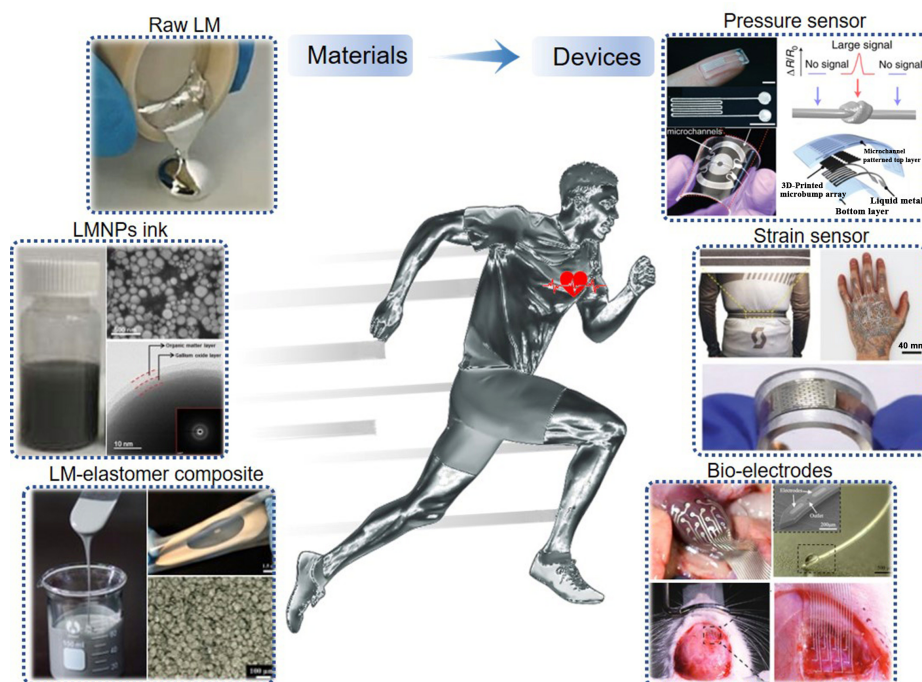


**Figure 1.** Schematic illustration depicting the LM-based materials for the preparation of flexible and wearable biosensors. LM: Liquid metal; LMNPs: LM nanoparticles.

To solve this problem, LMNP inks were developed as the patterning materials through sonicating bulk LMs in organic solvents, as shown in [Figure 2A](#) and [B](#). Acoustic cavitation generated by the probe induces the transformation of bulk LMs into LMNPs, while polymers containing anchoring groups, such as thiols, trithiocarbonate, phosphate, and silane, serve to colloiddally stabilize the LMNPs<sup>[20,37,49-53]</sup>. The particle size distribution of LMNP inks is associated with output power, sonication time, and solution temperature<sup>[50]</sup>. [Figure 2C](#) shows electron microscopy images and element mappings of LMNPs, demonstrating the core-shell structure with ~3 nm thick organic matter layers and amorphous Ga oxide layers. However, the existence of an oxide layer and cracks induced by the internal stress produced by unsymmetrical capillary forces make the circuit prepared by LMNP inks nonconductive [[Figure 2D](#)]<sup>[49]</sup>. In order to form a conductive pathway, sintering processes, such as mechanical sintering<sup>[49,54]</sup>, laser sintering<sup>[55,56]</sup>, and evaporation sintering<sup>[37]</sup>, should be used to break oxide shells of LMNPs for connecting fresh LM core. Li *et al.* proposed a method that differs from traditional methods, such as mechanical sintering and laser sintering, which are limited to rigid and heat-resistant substrates [[Figure 2E](#)]<sup>[57]</sup>. Instead, this method utilizes cellulose biological nanofibrils (CNFs) to achieve evaporative sintering of LMNP inks under ambient conditions. During the evaporation-induced sintering process, carbon nanofibrils (NFs) produce a local pressure that is large enough to rupture the oxide shell of LMNPs. As shown in [Figure 2F](#), the pattern after evaporation sintering under the ambient condition presents different optical refractive indices between the front and back of the pattern. Moreover, LMNP inks allow for inkjet printing to fabricate ultra-high-precision circuits. However, the grafting layer and the oxide reduce the electrical conductivity of sintered circuits.

### LM-elastomer composites

LM particles can be used as an ideal alternative to rigid fillers for making conductive composites. LM-elastomer composites combine the electrical, mechanical, and thermal properties of the filler and the elastomeric matrix<sup>[58-60]</sup>. The composite is usually prepared by shear mixing the precursor elastomer and LM,

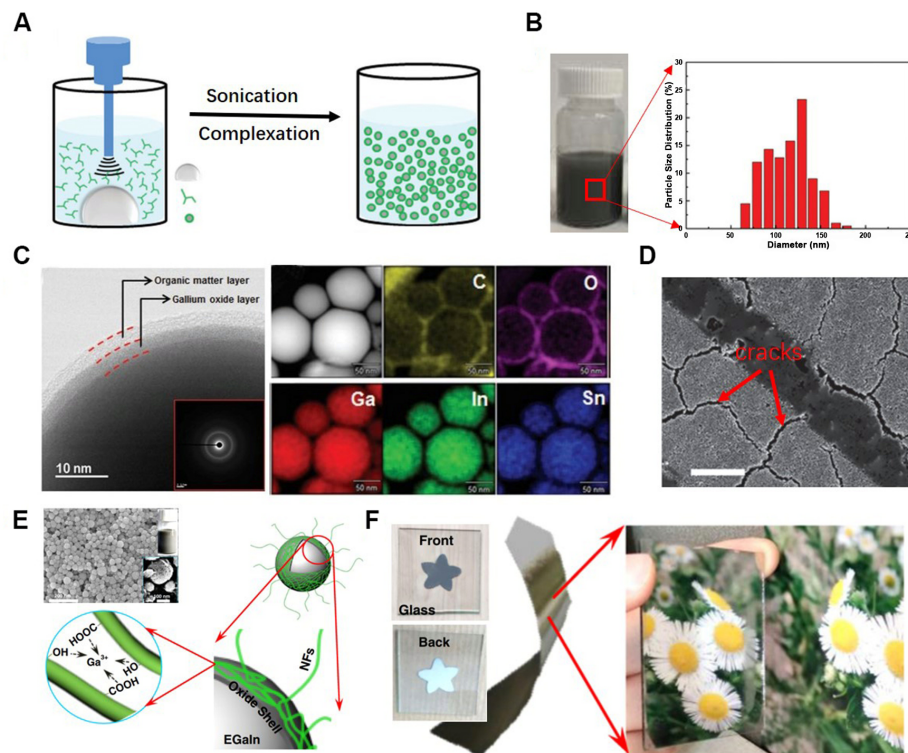


**Figure 2.** The fabrication method and microstructure characterization of LMNP inks. (A) Synthesize LMNPs by a probe sonication method. Reproduced with permission<sup>[50]</sup>. Copyright 2016, John Wiley and Sons; (B) Photo and particle size distribution of LMNP inks. Reproduced with permission<sup>[50]</sup>. Copyright 2016, John Wiley and Sons; (C) High Resolution Transmission Electron Microscope (HRTEM) and scanning transmission electron microscopy (STEM) images, along with elements mapping of LMNPs. Reproduced with permission<sup>[50]</sup>. Copyright 2016, John Wiley and Sons; (D) Scanning electron microscope (SEM) image of the circuit patterned using LMNP inks<sup>[49]</sup>. Scale bar is 20 m. Reproduced with permission. Copyright 2015, John Wiley and Sons; (E) Schematic illustration of EGaln droplets encapsulated in oxide shell and with CNFs attached on the surface via interactions with  $\text{Ga}^{3+}$ . Reproduced with permission<sup>[57]</sup>. Copyright 2019, The Authors; (F) Evaporation-induced sintering films with mirror-like bottom surface and grey top surface. Reproduced with permission<sup>[57]</sup>. Copyright 2019, The Authors. CNFs: Cellulose biological nanofibrils; EGaln: eutectic Ga-In; Ga: gallium; LM: liquid metal; LMNP: LM nanoparticle.

and the composite properties, such as conductivity and elastic modulus, can be regulated by the mixing time, mixing revolutions per minute (RPM), and curing temperature [Figure 3A and B]<sup>[61,62]</sup>. Compared to rigid fillers, LM fillers offer a composite with some unique electrical properties. For example, LM composites with the autonomously self-healing properties have been demonstrated [Figure 3C]<sup>[60]</sup>. When the composite is mechanically damaged, the droplets rupture to form new connections with neighboring droplets and restore the electrical function without human intervention or the application of external heat. Temperature-controlled reversible electrical transition between insulator and conductor properties has been achieved using LM fillers [Figure 3D]<sup>[63]</sup>. Upon freezing, the LM droplets within the composite undergo solidification and expand, establishing contact with one another to create conductive networks. Conversely, melting the filler material causes the composite to revert to an insulating state. Using both LM and solid metal particles as fillers to make hybrid composites endow the material with an unconventional positive piezoconductive property, whereby the conductivity increases exponentially upon stretching the material [Figure 3E]<sup>[64,65]</sup>. Such hybrid composites present great potential for wearable strain sensors, pressure-sensitive heating devices, and adjustable rheostat applications. In addition, LM inclusions also allow the adjustment of tensile modulus<sup>[66]</sup>, toughness<sup>[67]</sup>, electrical permittivity<sup>[68]</sup>, and thermal conductivity<sup>[58]</sup>. Owing to their remarkable performance, composites consisting of LMs and elastomers find extensive utility across a diverse spectrum of applications, including flexible and stretchable circuits, sensors, and electrical

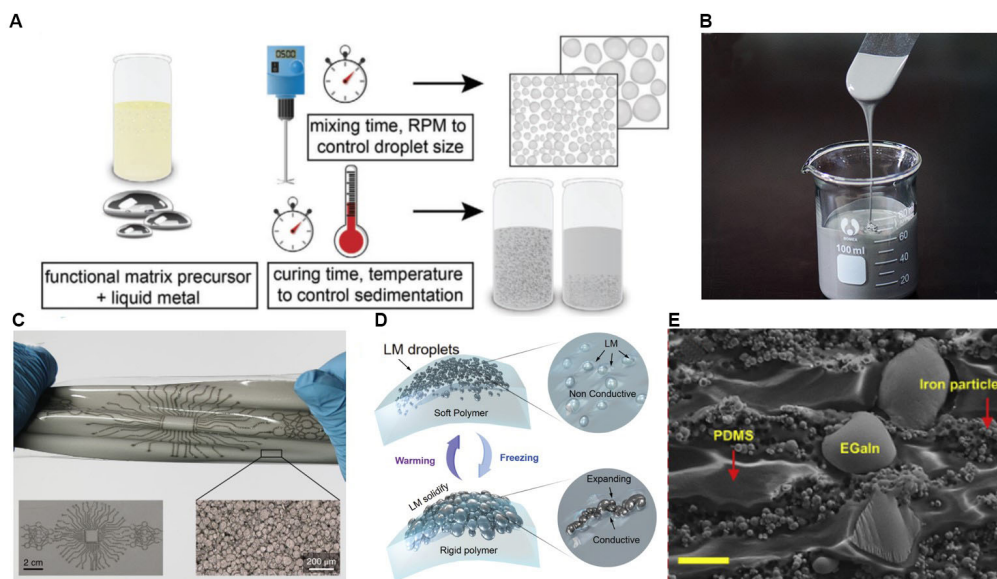


**Figure 3.** The preparation process and microstructure characterization of LM-elastomer composites. (A) The overview of processes for preparing LM inclusion composites. Reproduced with permission<sup>[61]</sup>. Copyright 2020, John Wiley and Sons; (B) Photograph of a kind of LM-elastomer composite for printing circuits. Reproduced with permission<sup>[62]</sup>. Copyright 2019, American Chemical Society; (C) An LM composite with self-healing performances being stretched and twisted. Reproduced with permission<sup>[60]</sup>. Copyright 2018, The Authors; (D) A schematic illustration of mechanisms in electrical transition between insulative and conductive LM composites to temperature change. Reproduced with permission<sup>[63]</sup>. Copyright 2019, John Wiley and Sons; (E) Microstructure characterization of LM-elastomer composites with anisotropic and unconventional piezoconductivity. Reproduced with permission<sup>[64]</sup>. Copyright 2020, Elsevier. EGaIn: Eutectic Ga-In; LM: liquid metal; PDMS: polydimethylsiloxane; RPM: revolutions per minute.

components. A systematic summary of LM-elastomer composites, including fabrication method and classification, can be found elsewhere<sup>[69,70]</sup>.

## WEARABLE BIOSENSORS

### Wearable interconnects

Interconnects are the most basic components for connecting electronic elements, such as sensors, resistors, and capacitors. High electrical conductivity, ease of patterning, high stretchability, and non-toxicity properties make LMs one of the best candidates for the fabrication of wearable circuits. Ga-based LMs in the forms of raw materials<sup>[71,72]</sup>, LM composites<sup>[70,73]</sup>, and LMNP inks<sup>[20,74]</sup> have been demonstrated to connect rigid electrical components. They can significantly improve the flexibility and electrical performance of wearable devices for healthcare applications, such as electrical stimulation, electrochemical sensing, and temperature monitoring.

Among raw LMs, LMNP inks, and LM composite materials, raw LMs are the most widely studied and used materials for the preparation of interconnects. For 3D-structured interconnects, LM fibers prepared by directly injecting raw LMs into microchannels have been applied for digital-embroidered electronic textiles<sup>[72]</sup>, magnetic resonance imaging (MRI) detectors<sup>[75]</sup>, and biomimetic eyes<sup>[76]</sup> [Figure 4A-C]. LM fibers are highly flexible and conductive, allowing them to be used in 3D spaces without any spatial constraints. This greatly expands the potential applications of LM circuits due to their adaptability to different environments. For 2D circuits, with the development of advanced patterning technologies<sup>[23]</sup>, the resolution of LM circuits has been significantly improved, which is of great significance in improving the integration of wearable devices. As shown in Figure 4D-F, LM interconnects with the widths of 250  $\mu\text{m}$ , 30  $\mu\text{m}$ , and even 500 nm can be prepared by injection<sup>[77-79]</sup>, transfer printing<sup>[80,81]</sup>, and lithography methods<sup>[82,83]</sup>, respectively. Interconnects prepared by raw LMs have metal-like electrical conductivity and outstanding stretchability,

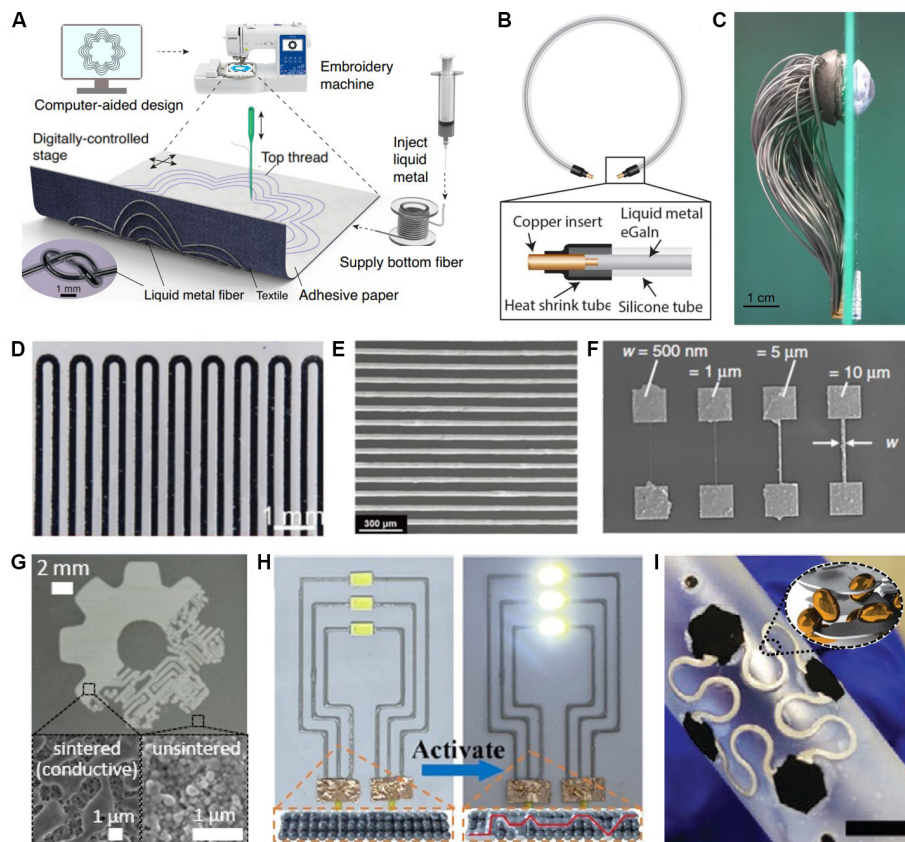


**Figure 4.** The circuits prepared using LM-based materials. (A) Digital-embroidered electronic textiles prepared by LM fibers. Reproduced with permission<sup>[72]</sup>. Copyright 2020, The Authors; (B) LM conductors for MRI detectors. Reproduced with permission<sup>[75]</sup>. The Authors; (C) Scheme of a biomimetic eye using LM fibers as the circuits. Reproduced with permission<sup>[76]</sup>. Copyright 2020, Springer Nature; LM circuits with the width of (D) 250  $\mu\text{m}$ . Reproduced with permission<sup>[78]</sup>. Copyright 2019, John Wiley and Sons; (E) 30  $\mu\text{m}$ . Reproduced with permission<sup>[81]</sup>. Copyright 2020, John Wiley and Sons and (F) 500 nm. Reproduced with permission<sup>[82]</sup>. Copyright 2020, The Authors; (G) Circuits prepared using LMNP inks and sintered by laser. Reproduced with permission<sup>[55]</sup>. Copyright 2018, American Chemical Society; (H) The circuits prepared using LM composite before and after the activation. Reproduced with permission<sup>[85]</sup>. Copyright 2021, American Chemical Society; (I) LM composite circuits for “island-bridge” structure of an energy harvesting system<sup>[86]</sup>, scale bar is 5 mm. Reproduced with permission. Copyright 2020, John Wiley and Sons. LM: Liquid metal; LMNP: LM nanoparticle; MRI: magnetic resonance imaging.

and the stretchability is only limited by the elastomer that encapsulates LMs. On the other hand, the use of bulk LMs may present challenges as it is susceptible to leakage. In addition, establishing a reliable connection with electronic components can be challenging as the LM must be able to effectively wet the surface of the component<sup>[84]</sup>. Therefore, LMNP inks and LM composites have been developed for the fabrication of interconnects, which can significantly enhance the wettability to form good connections. Compared to raw LM materials, LMNP inks have the advantages of compatibility with diverse substrates and ease of scalability and allow for automatic fabrication methods. For example, Liu *et al.* proposed a spray-printing strategy for the scalable fabrication of soft and flexible circuits based on a LMNP ink, but an additional sintering process is needed to rupture and ablate the LMNP  $\text{Ga}_2\text{O}_3$  shell to allow the LM cores to escape and coalesce [Figure 4G]<sup>[55]</sup>.

LM-elastomer composites can further be used to enhance the working reliability of LM interconnects [Figure 4H and I]<sup>[85,86]</sup>. On the one hand, LM-elastomer composites can improve the surface wettability of the patterned interconnects on diverse substrates. On the other hand, the bond between LM-elastomer

composites and flexible substrates could be stronger. For example, circuits prepared by LM-Polydimethylsiloxane (PDMS) composites can be integrated into PDMS substrates after curing, which can significantly improve the working reliability. Since LMs are dispersed in the elastomer in the form of microparticles, the risk of bulk LM leakage can be reduced. Similar to LMNP inks, LM-elastomer interconnects should be activated by additional processes such as pressing or freezing<sup>[85,87]</sup>. By adding some rigid materials, such as copper<sup>[88,89]</sup>, silver<sup>[86,90]</sup>, and nickel<sup>[91]</sup> particles, in an LM-elastomer composite, the interconnects can be actively activated through the extrusion effect of rigid particles when it is subjected to a stretching state. Attributed to the non-leaking performance and excellent biocompatibility of LM-elastomer composites, we believe that interconnects prepared using LM-elastomer composites have broader prospects in wearable electronics.

### Wearable sensors

Wearable sensors affixed to garments or directly onto the human skin have emerged as crucial tools for real-time activity monitoring. Wearable devices necessitate highly reliable sensors that can conform to the curvilinear surface of the human body with minimal discomfort. LM-based materials are outstanding candidates for preparing wearable sensors due to their fluidic nature and biocompatibility. Due to the fluidity of LMs and low elastic modulus of encapsulating polymers, LM channels inside the polymer can be deformed upon the application of external forces, inducing the change of electrical signals. LM-based flexible and wearable sensors have recently demonstrated immense potential for various applications, including healthcare monitoring<sup>[23,92]</sup>, disease early warning<sup>[93]</sup>, motion detection<sup>[26,62,94,95]</sup>, and soft robotics<sup>[96]</sup>. These sensors, particularly stretchable and skin-mountable variants, can function as pressure, strain, optical, and temperature sensors, as elaborated in detail below.

**Pressure Sensors:** Wearable LM-based pressure sensors commonly use resistance or capacitance-based detection methods to sense pressure changes. Most LM pressure sensors detect the change of resistance. The LM encapsulated within a fluid channel deforms when an external force is applied to it [Figure 5A and B]<sup>[79,97]</sup>, leading to the change in cross-sectional area. Consequently, the resistance of the sensor changes. For capacitive-based pressure sensors, the sensing mechanism mainly depends on detecting the change in the thickness of the dielectric layer or the overlapping area between the LM and the underlying electrode<sup>[98-101]</sup>. The utilization of LM pressure sensors in devices for detecting pulse rate, footsteps, and tactile feedback has shown great potential in biomedical applications [Figure 5C]<sup>[23,25,102-105]</sup>.

The sensitivity of a sensor is a critical parameter for sensing applications, and research has demonstrated that the Poisson's ratio of the material, the thickness of the top layer, and the dimension of microchannels all play significant roles in the sensitivity of microchannel-based pressure sensors<sup>[106,107]</sup>. The pressure sensitivity of previously reported LM-based pressure sensors is within the range of  $0.2\text{-}80 \times 10^{-3} \text{ kPa}^{-1}$ , and such sensitivity is not optimal due to the relatively thick elastomer dielectric layer<sup>[103]</sup>. Therefore, strategies, such as microchannel cross-sectional geometry design for enhancing the penetrating effect of channel base<sup>[108]</sup>, 'S'-shaped microfluidic structure design with a higher and sharper deformation profile<sup>[102]</sup>, and Wheatstone bridge circuit design<sup>[23]</sup>, have been proposed to improve the sensitivity. Kim *et al.* introduced 3D-printed rigid microbumps on the top of an LM microchannel that can offer extremely high sensitivity ( $0.158 \text{ kPa}^{-1}$ ) compared with traditional straight channel LM pressure sensors ( $0.2\text{-}80 \times 10^{-3} \text{ kPa}^{-1}$ ), as shown in Figure 5D<sup>[103]</sup>. Furthermore, a low-cost and highly-sensitive LM pressure sensor for gastrointestinal manometry was prepared to refer to the quipu-knotted strings, as shown in Figure 5E<sup>[109]</sup>. By simply typing knots on the EGaIn-filled fiber, a small pressure of less than 50 kPa can be detected, while no signal can be detected when the same pressure is applied to the unknotted region. The enhanced sensitivity is attributed to the amplification of the effective total pressure induced by the folded and stacked channel layers. For application demonstration, the designed ribbon-like manometry device with eight knots can clearly record

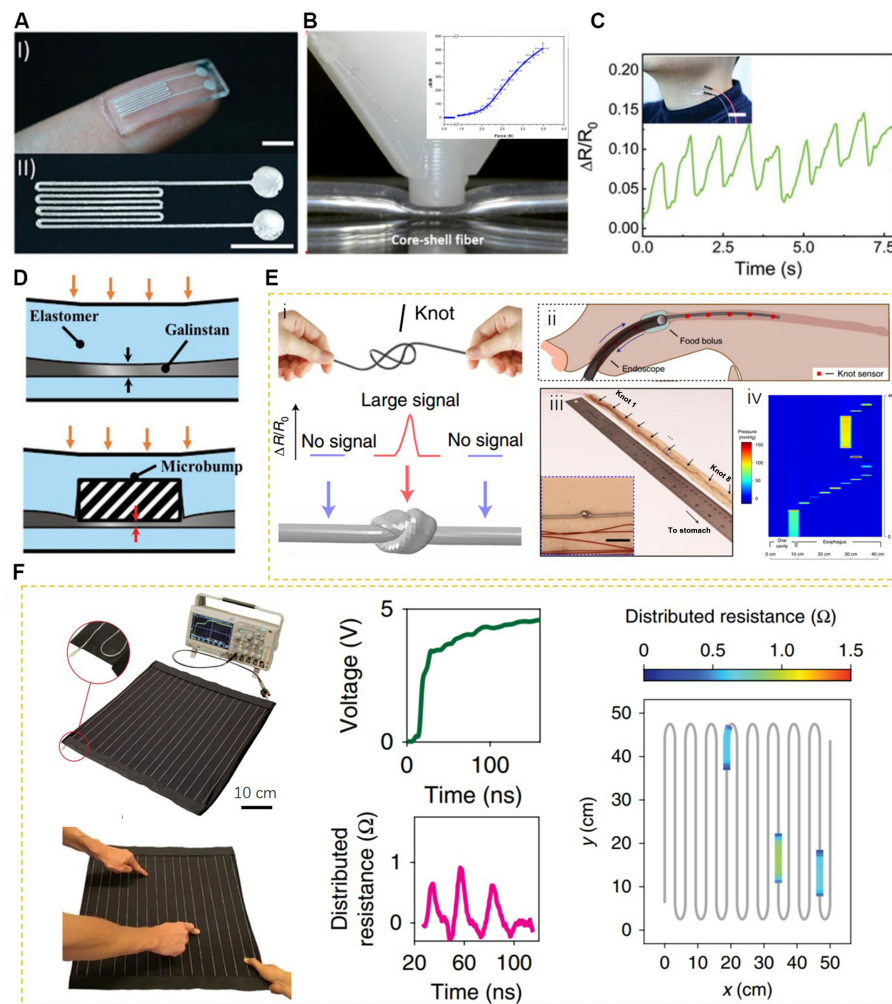


**Figure 5.** Pressure sensors prepared using LMs; (A) Photograph of the pressure sensor prepared by a channel filling method, scale bars are 5 mm. Reproduced with permission<sup>[97]</sup>. Copyright 2019, John Wiley and Sons; (B) Photograph for testing the performance of a fiber-structured pressure sensor, and the insert is the resistance change  $R/R_0$  under different force loadings. Reproduced with permission<sup>[79]</sup>. Copyright 2020, Elsevier B.V.; (C) The resistance change of LM pressure sensors prepared by channel filling method for monitoring human neck pulses. Reproduced with permission<sup>[97]</sup>. Copyright 2019, John Wiley and Sons; (D) Schematic illustration of the highly sensitive pressure sensor enhanced by a rigid micropump. Reproduced with permission<sup>[103]</sup>. Copyright 2019, John Wiley and Sons; (E) Enhanced sensitivity of LM pressure sensors by resembling the quipu-knotted strings used by Andean civilizations for monitoring the gastrointestinal pressure. Reproduced with permission<sup>[109]</sup>. Copyright 2022, Springer Nature; (F) Soft and stretchable LM transmission lines as distributed probes of multimodal deformations. Reproduced with permission<sup>[113]</sup>. Copyright 2020, Springer Nature. LM: Liquid metal.

the backflow and retention of artificial food bolus by evaluating the oesophageal pressure [Figure 5E ii and iii].

Quantifying and spatially sensing dynamic multipoint deformations remain a challenge. Skin-like multi-tactile sensors have shown significance for acquiring tactile information of multiple points<sup>[110-112]</sup>. For LM-based multi-tactile sensors, a two-layer core-shell fiber-based tactile sensor has been designed and fabricated via the coaxial ink writing of a continuous single core-shell fiber<sup>[79]</sup>. When two fingers are placed on the two sensing nodes, the resistances of both the top and bottom layer fibers of the sensing nodes are simultaneously recorded. The resistance values can be used to determine the specific position of the fingers. Furthermore, based on time-domain reflectometry, Leber *et al.* proposed a soft and stretchable LM

transmission line as distributed probes for sensing multimodal deformations, as shown in Figure 5F<sup>[113]</sup>. In this sensor, soft transmission line probes were integrated into a piece of stretchable fabric, and a custom pulse generator was used in conjunction with a standard laboratory oscilloscope to induce time-domain reflection. When the transmission line is pressed, steps of signal appear in the waveform and peaks equal to the number of pressed points emerge in the distributed resistance profile, the height of which corresponds to the applied pressure. These points can then be accurately positioned on the spatial map.

**Strain Sensors:** Similar to LM pressure sensors, sensors based on the change of resistance<sup>[114,115]</sup>, capacitance<sup>[116]</sup>, and resonant frequency<sup>[117]</sup> have been employed to detect strain. For LM-filled fiber and microchannel strain sensors, LM elongates along the strain direction, leading to an increase of resistance that conforms to the equation  $R = R_0 (1 + \varepsilon)^2$  ( $R_0$ : initial resistance,  $\varepsilon$ : strain,  $R$ : the resistance corresponds to  $\varepsilon$ ). For most applications, these types of strain sensors are integrated into wired/wireless gloves to detect hand gestures by monitoring the output voltage or resistance in real-time<sup>[25,26,48,87,114]</sup>. Tang *et al.* developed a layer-by-layer fabrication method for integrating strain sensors with a multilayer electronic transfer tattoo that can be stretched up to 800% strain and conformably attached to the skin [Figure 6A]<sup>[118]</sup>. This tattoo can amplify the output signal of integrated strain sensors by three times and achieve the monitoring of hand movements in real time [Figure 6B]. In addition, Dong *et al.* proposed a fiber strain sensor with a surface texture and six LM electrodes to realize the breath monitoring based on self-powered sensing [Figure 6C]<sup>[92]</sup>. The strain sensor LM consisted of fiber extremities fixed to the two ends of a longer stretchable belt. During respiration, the movement of the abdomen caused friction between the belt and the fiber, resulting in a slight relative movement that generated an electrical signal. This signal can be detected to evaluate the inward and outward movements of the upper chest and abdomen [Figure 6C iv].

The gauge factor (GF), which reflects the sensitivity of the LM-based straight channel strain sensor, is relatively low (below 5 under 100% strain). Theoretically, the relatively low average GF of a straight-channel strain sensor, as described by the formula  $GF = \varepsilon + 2$ , fails to meet the criteria set for commercial wearable strain sensors. To increase the sensitivity, Kramer *et al.* introduced a curvature sensor with a hollow structure, in which an embedded strut can exert pressure on the microchannel during bending, leading to a greater change in resistance<sup>[119]</sup>. Moreover, a nacre-inspired and LM-based ultrasensitive strain sensor by a spatially regulated cracking strategy has been developed [Figure 6D i and ii]<sup>[94]</sup>. The biphasic pattern (LM with Cr/Cu underlayer) acts as “bricks”, and strain-sensitive Ag film acts as “mortar”. Compared to LM conductors, this strategy allows the conductive pathways to form a certain number of cracks under strain [Figure 6D iii]; thereby, the sensitivity was increased by two orders of magnitude [Figure 6D iv]. In addition, Li *et al.* designed a highly sensitive LM strain sensor based on strain redistribution and 3D-structured circuit strategies [Figure 6E]<sup>[120]</sup>. In the middle of the strain sensor, a high-elastic-modulus cuboid elastomer (E650) is wound with the Ga-10In solid wire [Figure 6E i]. When the sensor is stretched, the cuboid elastomer squeezes the LM channel to reduce its cross section, further increasing the sensitivity [Figure 6E ii]. The average GF of 100% strain is improved more than 400 times compared with the previously reported 2D LM strain sensor [Figure 6E iii]. Generally, the channel structure design strategy and strain redistribution strategy can lead to a more significant resistance change under a small strain.

**Temperature sensors:** Temperature is a critical and fundamental parameter to evaluate human health. The volume expansion of fluid in a closed pipe correlated to a specific temperature value is a commonly used principle in thermometers, as seen in the traditional mercury thermometer. In contrast to mercury-based thermometers, the preminent merit of Ga-based thermometers for wearable biosensors is their neglected toxicity. This remarkable trait, coupled with their supercooling performance, empowers Ga-based thermometers-founded upon the principle of volume expansion-to reliably operate in environments as

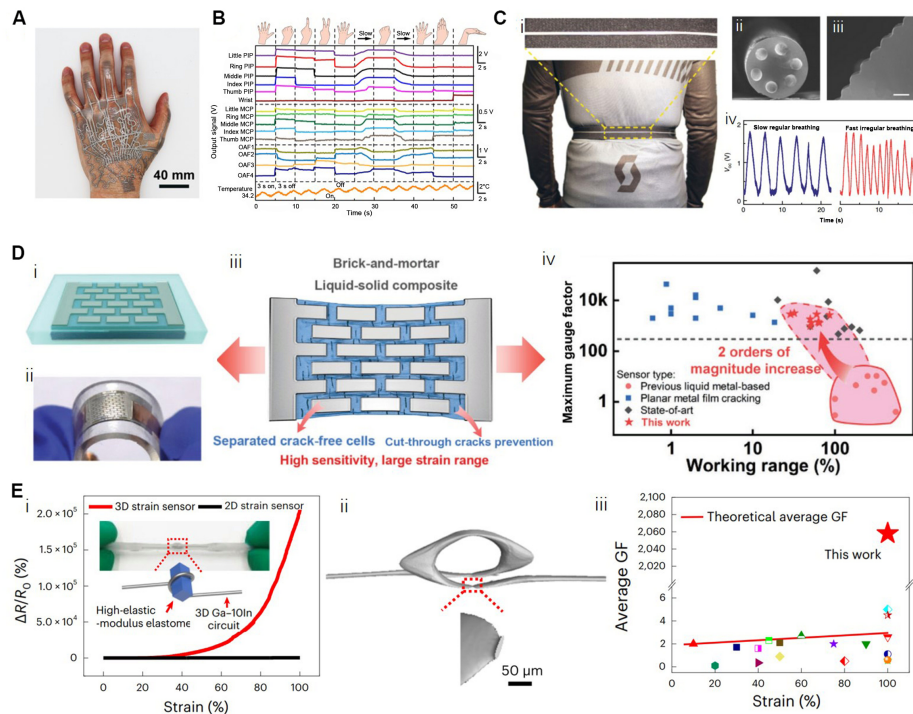


**Figure 6.** LM-based strain sensors. (A and B) An LM-based multilayer tattoo integrated with stretchable strain sensors can precisely monitor the hand movements in real time. Reproduced with permission<sup>[118]</sup>. Copyright 2021, American Association for the Advancement of Science; (C) Breathing monitoring by a self-powered triboelectric fiber featured strain sensor with six embedded electrodes and surface texture. Reproduced with permission<sup>[92]</sup>. Copyright 2020, Springer Nature; (D) LM-based and nacre-inspired strain sensors, the brick-and-mortar architecture can control the micrograph of cracks; thus, the sensitivity was increased by about two orders of magnitude. Reproduced with permission<sup>[94]</sup>. Copyright 2021, John Wiley and Sons; (E) Resistance response, microstructure characterization, and sensitivity comparison of a high-sensitive 3D-structured LM strain sensor. Reproduced with permission<sup>[120]</sup>. Copyright 2023, All authors. Ga: Gallium; GF: gauge factor; LM: liquid metal.

frigid as  $-5\text{ }^{\circ}\text{C}$  and, in some cases, even down to  $-10\text{ }^{\circ}\text{C}$ . Evidencing their practicality, medical-grade Ga-based thermometers from esteemed manufacturers, such as Geratherm and Mediblink, have gained substantial traction in commercial utilization.

The Seebeck effect is another commonly used principle for designing and fabricating thermometers in the industry<sup>[121,122]</sup> and occurs when the ends of a thermocouple are subjected to a temperature difference, resulting in an electrical current flowing between them. Thermometers prepared based on the Seebeck effect exhibit much higher sensitivity compared to those utilizing the volume expansion principle<sup>[107]</sup>. Li *et al.* prepared a thermocouple using Ga and EGaIn as the materials of two branches, respectively [Figure 7A i]<sup>[123]</sup>. By utilizing the setup shown in Figure 7A ii, the temperature sensor exhibits a good linear correlation between thermoelectric voltage and the temperature in the range of  $0\sim 200\text{ }^{\circ}\text{C}$ . The accuracy of the thermocouples is  $\pm 0.5\text{ }^{\circ}\text{C}$ , but the Seebeck coefficient is limited to  $0.14\text{ }\mu\text{V}/^{\circ}\text{C}$  [Figure 7A iii]. Furthermore, Wang *et al.* developed a handy flexible micro-thermocouple by injecting bismuth/Ga-based mixed alloys into microchannels [Figure 7B i]<sup>[124]</sup>. A small microchannel was fabricated near the sensing area to vent the air from the microchannel and allowed EGaInSn to overflow from the small microchannel [Figure 7B ii]. The experimental results suggest that the Seebeck coefficient of the thermometer is about  $-10.54\text{ }\mu\text{V}/^{\circ}\text{C}$  [Figure 7B iii], which is much higher than the temperature sensor given in Figure 7A. A higher Seebeck coefficient of the temperature sensor is due to the presence of Bi-based alloys in the mixture. However, it should be noted that an increase in the Bi-based alloy content can make the sensor more

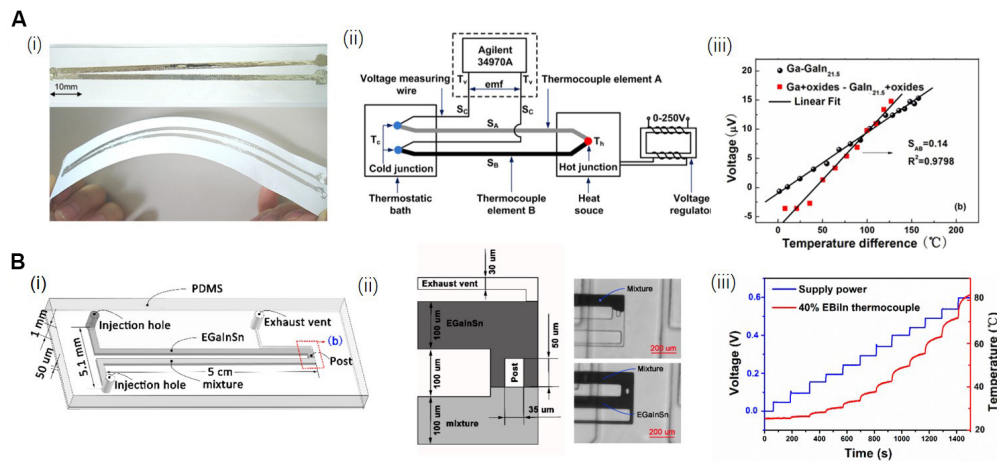


**Figure 7.** Temperature sensors designed and prepared using the LMs. (A i) Photograph of the printed thermocouple prepared using Ga with 0.25 wt.% oxides- GaIn<sub>21.5</sub> with 0.25 wt.% Ga oxides, and the thin film thickness is about 50  $\mu\text{m}$ ; (A ii) Schematic diagram of a printable tiny thermocouple prepared by LMs; (A iii) The measured thermoelectric voltage as a function of temperature difference using the thermocouple in (A i). Reproduced with permission<sup>[123]</sup>. Copyright 2012, AIP publishing; (B i) Schematic of a handy micro-thermocouple, two poles of the channel are filled with EGalnSn and Bi-based metal-alloy mixture, respectively; (B ii) The EGalnSn and mixture converged at the middle of the channel; (B iii) Performance of the thermocouple in (B i). Reproduced with permission<sup>[124]</sup>. Copyright 2019, Multidisciplinary Digital Publishing Institute. EGaln: Eutectic Ga-In; Ga: gallium; PDMS: polydimethylsiloxane.

susceptible to damage when bent. Therefore, the thermocouple with a 40% mass ratio of EBIn was used for the temperature sensor. This type of temperature sensor is flexible due to the fluidic nature of Ga-based LMs, which could be beneficial for long-term wearing.

### Implantable bioelectrodes

Ga-based LMs have shown great potential for bio-related applications due to their excellent electrical conductivity, fluidic properties, and negligible toxicity. Reports suggest that LMs can be directly patterned onto the skin for ECG monitoring<sup>[125-127]</sup>, fabricated into external stents and electronic blood vessels<sup>[128,129]</sup>, and acted as nerve connectors<sup>[130]</sup>. Despite the promising properties of LM-based stretchable and implantable electronics, there are still practical issues that need to be addressed. One major concern is the fluidic nature of LMs, which can lead to insufficient structural stability when in direct contact with dynamically moving organs and tissues. This lack of stability can compromise the security and reliability of the electronics. One approach to solve this problem is to alter the rheology of LMs by increasing the content of In in a Ga-In alloy. For instance, Timosina *et al.* reported that the Ga-In alloy with 50 wt% of In has a non-Newtonian shear-thinning property, exhibiting high viscosity when still, and can flow similarly to an LM when sheared<sup>[127]</sup>. This property can prevent material leakage and enhance processability. Also, the rapid formation of an insulating Ga<sub>2</sub>O<sub>3</sub> layer severely affects the conductive performance between LMs and tissues. Another challenge with using LMs for long-term service in bioelectronics applications is their susceptibility to chemical corrosion under physiological conditions. This presents significant challenges to the efficiency and safety of the devices. To address this issue, LMs are often encapsulated in bio-friendly polymers for flexible bioelectronics applications. By using LMNPs, Dong *et al.* proposed an LM electrode array prepared using the screen-printing method for *in vivo* neural recording<sup>[131]</sup>. In addition, by utilizing the low melting point property of pure Ga, a flexible and multifunctional neural probe with ultra-large tunable stiffness for deep-brain chemical sensing and agent delivery has been developed, as shown in Figure 8A<sup>[132]</sup>. This neural probe was designed with three layers, and pure Ga LMs were used to fill the top stiffening channel layer and medium conductive channel. At room temperature, the neural probe is stiff due to the solid state of pure Ga. When the probe is inserted into the brain, the body temperature will induce the melting of Ga so that the neural electrodes restore flexibility [Figure 8B].

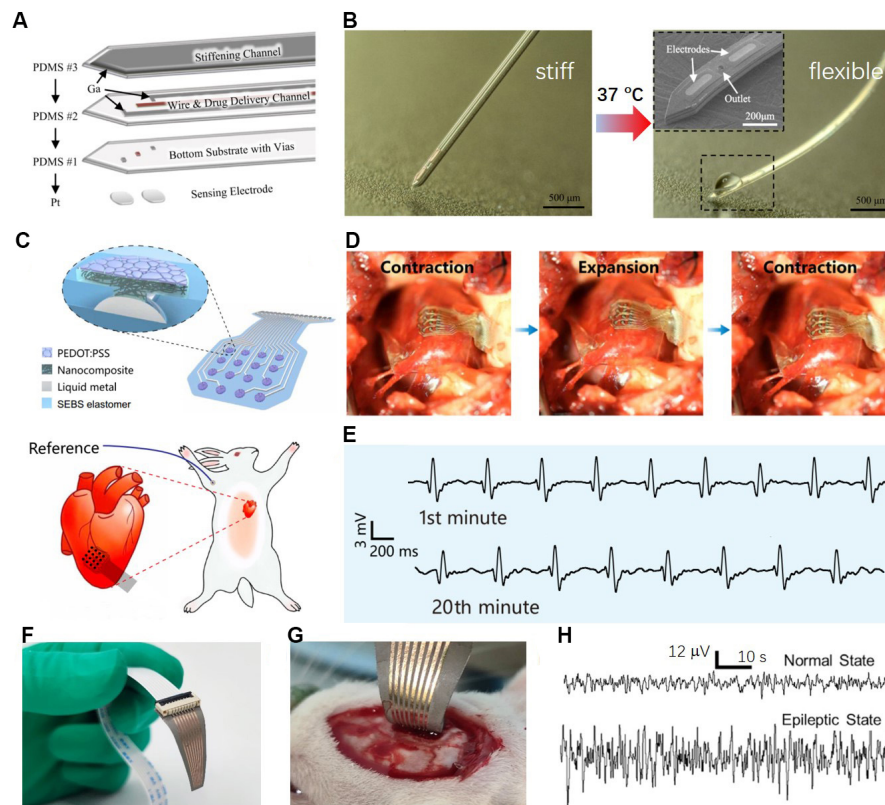


**Figure 8.** Implantable flexible electrodes for sensing biosignals. (A) The exploded-view drawing of the ultra-large tunable stiffness electrodes enabled by LMs. Reproduced with permission<sup>[132]</sup>. Copyright 2019, Elsevier B.V.; (B) The stiff state electrode can translate into soft state due to the melting of LMs, and the insert picture shows the outlet of the drug delivery channel and Pt electrodes of the probe tip. Reproduced with permission<sup>[132]</sup>. Copyright 2019, Elsevier B.V.; (C) Schematic illustration of the highly stretchable electrodes for *in vivo* epicardial recording on a rabbit. Reproduced with permission<sup>[134]</sup>. Copyright 2022, American Association for the Advancement of Science; (D) The electrodes can be conformally attached to the right ventricle for long-term monitoring of the electrocardio; and (E) shows the representative electrogram for 20 min of monitoring. Reproduced with permission<sup>[134]</sup>. Copyright 2022, American Association for the Advancement of Science; (F) Photo of the stretched neural electrode arrays prepared by depositing Au film on LM-PDMS composite. Reproduced with permission<sup>[135]</sup>. Copyright 2022, All authors; (G) Intraoperative image of the neural electrode arrays for *in vivo* recording of ECoG signals, showing the high flexibility of the electrode to be in contact with the cerebral cortex of the rat; and (H) ECoG signals of a healthy rat under normal state and epileptic state. Reproduced with permission<sup>[135]</sup>. Copyright 2022, All authors. ECoG: Electrocardiogram; LM: liquid metal; PDMS: polydimethylsiloxane; PEDOT:PSS: poly 3,4-ethylene dioxythiophene : polystyrene sulfonate; SEBS: styrene-ethylene-butylene-styrene.

Although electrode arrays show stable electrical properties under high strain, the deposited solid-state conductors at the sensing site significantly affect the long-term stability due to the mechanical mismatch of the interface between the metal and polymer. Therefore, deposited conductive polymers have been adapted to encapsulate LM interconnects inside the polymer<sup>[133,134]</sup>. Wang *et al.* selected carbon nanotube composites and microcracked conductive poly 3,4-ethylene dioxythiophene : polystyrene sulfonate (PEDOT:PSS) polymer as the sensing sites of electrodes, as shown in Figure 8C<sup>[134]</sup>. Combining LM interconnects with a highly stretchable styrene-ethylene-butylene-styrene (SEBS) elastomer allows the electrode array to exhibit ultrahigh stretchability (up to 400% tensile strain) and a low interfacial impedance. In addition, the long-term *in vivo* epicardial recording on a rabbit [Figure 8D and E] further demonstrates the vast potential of the electrodes for health monitoring applications. Li *et al.* fabricated a stretchable 8-channel neural electrode array by depositing an Au film onto the surface of an LM-PDMS composite [Figure 8F]<sup>[135]</sup>. The electrode array can conformally match the cortical surface of a rat due to its high flexibility and stretchability [Figure 8G]. The electrode array was effectively utilized for the *in vivo* identification of epilepsy by

monitoring electrocorticogram (ECoG) signals [Figure 8H]. However, there is still a risk of leakage of raw LMs in implantable bioelectrodes. Therefore, we propose that implantable bioelectrodes based on LM-elastomer composites should be given more attention in future research, as they have the potential to address the issue of LM leakage.

## CONCLUSIONS AND OUTLOOKS

Unique properties such as fluidity, metallic electrical/thermal conductivity, and low toxicity of LMs contribute to their broadening applications of biosensors in the healthcare area. This review illustrated the recent advances in flexible and wearable LM-based biosensors, including interconnects, pressure sensors, strain sensors, temperature sensors, and implantable electrodes. However, there remain some challenges and opportunities associated with Ga-based biosensors, which are shown in Figure 9 and summarized below:

(1) Despite that many works have reported the low cytotoxicity of Ga and its alloys, it deserves to be noted that some reports revealed that Ga-based LMs are toxic at the cellular level<sup>[136,137]</sup>, and the threshold concentrations of Ga, Ga-based alloys, and Ga ions need to be systematically investigated by conducting *in vitro/vivo* experiments. An important consideration when using bulk Ga-based LMs in biomedical applications is whether the Ga ions released from these materials can be absorbed through the skin<sup>[127]</sup>. In addition, further research is needed to investigate the metabolic process and potential toxicity mechanisms of Ga ions in the body<sup>[138]</sup>. For instance, further investigations are warranted to elucidate the mechanism by which Ga ions induce damage to normal cellular components.

(2) Advanced connection technologies should be further developed to connect flexible LM biosensors to rigid electrical components. Currently, most LM-based biosensors use rigid metal wires to connect the encapsulated LM patterns with the external printed circuit board. However, the soft-rigid connection between the LM patterns and the wires is a weak point due to the mechanical mismatch between the two materials. For example, the rigid metal wire is very easy to be pulled out from the polymer. Besides, LMs would leak along the interface between the rigid metal wire and polymer while the biosensor is under long-term usage. Therefore, it is urgent to develop a more reliable encapsulation method to connect LM patterns and rigid electrical components. We recommend that the conductive LM-elastomers possess the potential to address the connection problem.

(3) The fluidic nature of LMs makes them susceptible to leakage from the encapsulating polymer, which can lead to contamination. This risk is exacerbated by stress concentrations generated by external forces during long-term stretching or folding. The leaked Ga-based LM can solder with electrical components without heating, which is destructive for electronic circuits. To prevent leakage of LM during long-term usage, effective encapsulation measures should be taken. Additionally, controlling the fluidity and wettability of LMs through oxidation, mixing with solid metal microparticles, and the development of novel LM-elastomer composites are effective strategies to address this problem.

(4) The resolution of LM-based biosensor patterns is another area that requires attention. Although LM nano-patterns with ~500 nm line width have been fabricated using lithography, the resolution is relatively lower than that achievable on a silicon wafer. High resolution is crucial for the integration of LM-based biosensors into flexible electronics. Therefore, future research should focus on developing precision instruments and optimizing processes, such as oxide formation and phase transition, during the patterning process to improve the resolution of LM patterns.

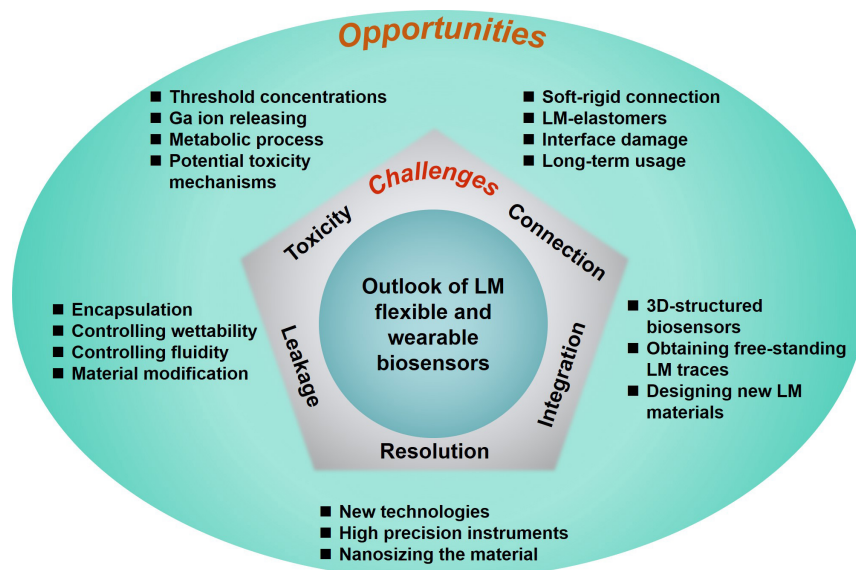


**Figure 9.** Prospects for challenges and opportunities in Ga-based wearable biosensors. Ga: Gallium; LM: liquid metal.

(5) One last issue that needs to be considered is the integration of LM-based biosensors. In addition to increasing the LM patterns resolution, fabricating 3D-structured biosensors is another effective solution to improve the integration of biosensors. However, obtaining free-standing LM traces and stable interconnects is challenging due to the fluidity of LMs. The commonly used microchannel filling methods and 3D printing methods cannot meet the requirements of efficient fabrication of highly integrated biosensors. We believe it is necessary to design new LM materials, such as alloys with plastic deformation performance, to develop a highly efficient fabrication method for highly integrated LM biosensors. In addition, creating multifunctional 3D printing holds a prominent advantage for achieving high precision and integrated 3D-structured biosensors.

## DECLARATIONS

### Authors' contributions

Initiated the reviewing idea and outlined the manuscript structure: Xu Z, Ma X, Guo J

Involved in the discussion and revised the manuscript: Tang SY

Conducted the literature review and wrote the manuscript draft: Li G, Liu S

All authors have read the manuscript and approved the final version.

### Availability of data and materials

Not applicable.

### Financial support and sponsorship

This work was supported by the Engineering and Physical Sciences Research Council (EPSRC) grant (EP/V008382/1), the National Natural Science Foundation of China (92163109), Shenzhen Science and Technology Program (KQTD20170809110344233), and the Fundamental Research Funds for the Central Universities (Grant No. HIT.OCEF.2021032).

### Conflicts of interest

All authors declared that there are no conflicts of interest.

### Ethical approval and consent to participate

Not applicable.

### Consent for publication

Not applicable.

### Copyright

© The Author(s) 2023.

## REFERENCES

1. Ma B, Xu C, Chi J, Chen J, Zhao C, Liu H. A versatile approach for direct patterning of liquid metal using magnetic field. *Adv Funct Mater* 2019;29:1901370. DOI
2. Zhou X, Zhang Y, Yang J, Li J, Luo S, Wei D. Flexible and highly sensitive pressure sensors based on microstructured carbon nanowalls electrodes. *Nanomaterials* 2019;9:496. DOI PubMed PMC
3. Jiang Y, Liu Z, Matsuhisa N, et al. Auxetic mechanical metamaterials to enhance sensitivity of stretchable strain sensors. *Adv Mater* 2018;30:e1706589. DOI
4. Li H, Xu Y, Li X, et al. Epidermal inorganic optoelectronics for blood oxygen measurement. *Adv Healthc Mater* 2017;6:1601013. DOI
5. Jiao B. Anti-motion interference wearable device for monitoring blood oxygen saturation based on sliding window algorithm. *IEEE Access* 2020;8:124675-87. DOI
6. Liu Z, Qi D, Hu G, et al. Surface strain redistribution on structured microfibers to enhance sensitivity of fiber-shaped stretchable strain sensors. *Adv Mater* 2018;30:1704229. DOI
7. Liao X, Zhang Z, Kang Z, Gao F, Liao Q, Zhang Y. Ultrasensitive and stretchable resistive strain sensors designed for wearable electronics. *Mater Horiz* 2017;4:502-10. DOI
8. Zhang M, Wang C, Wang H, Jian M, Hao X, Zhang Y. Carbonized cotton fabric for high-performance wearable strain sensors. *Adv Funct Mater* 2017;27:1604795. DOI
9. Maier D, Laubender E, Basavanna A, et al. Toward continuous monitoring of breath biochemistry: a paper-based wearable sensor for real-time hydrogen peroxide measurement in simulated breath. *ACS Sens* 2019;4:2945-51. DOI PubMed PMC
10. Veeralingam S, Khandelwal S, Sha R, Badhulika S. Direct growth of FeS<sub>2</sub> on paper: a flexible, multifunctional platform for ultra-low cost, low power memristor and wearable non-contact breath sensor for activity detection. *Mat Sci Semicon Proc* 2020;108:104910. DOI
11. Liu Z, Wang H, Huang P, et al. Highly stable and stretchable conductive films through thermal-radiation-assisted metal encapsulation. *Adv Mater* 2019;31:1901360. DOI
12. Jeong YR, Lee G, Park H, Ha JS. Stretchable, skin-attachable electronics with integrated energy storage devices for biosignal monitoring. *Acc Chem Res* 2019;52:91-9. DOI
13. Wei C, Tan L, Tao Y, et al. Interfacial passivation by room-temperature liquid metal enabling stable 5 V-class lithium-metal batteries in commercial carbonate-based electrolyte. *Energy Stor Mater* 2021;34:12-21. DOI
14. Wei C, Tan L, Zhang Y, et al. Highly reversible Mg metal anodes enabled by interfacial liquid metal engineering for high-energy Mg-S batteries. *Energy Stor Mater* 2022;48:447-57. DOI
15. Dickey MD. Stretchable and soft electronics using liquid metals. *Adv Mater* 2017;29:1606425. DOI PubMed
16. Zhu S, So J, Mays R, et al. Ultrastretchable fibers with metallic conductivity using a liquid metal alloy core. *Adv Funct Mater* 2013;23:2308-14. DOI
17. Dickey MD, Chiechi RC, Larsen RJ, Weiss EA, Weitz DA, Whitesides GM. Eutectic Gallium-Indium (EGaIn): a liquid metal alloy for the formation of stable structures in microchannels at room temperature. *Adv Funct Mater* 2008;18:1097-104. DOI
18. Yang X, Tan S, Liu J. Numerical investigation of the phase change process of low melting point metal. *Int J Heat Mass Transf* 2016;100:899-907. DOI
19. Liu S, Sweatman K, McDonald S, Nogita K. Ga-based alloys in microelectronic interconnects: a review. *Materials* 2018;11:1384. DOI PubMed PMC
20. Zhang M, Li G, Huang L, et al. Versatile fabrication of liquid metal nano-ink based flexible electronic devices. *Appl Mater Today* 2021;22:100903. DOI
21. Sun X, Cui B, Yuan B, et al. Liquid metal microparticles phase change mediated mechanical destruction for enhanced tumor cryoablation and dual-mode imaging. *Adv Funct Mater* 2020;30:2003359. DOI
22. Gao Q, Li H, Zhang J, Xie Z, Zhang J, Wang L. Microchannel structural design for a room-temperature liquid metal based super-stretchable sensor. *Sci Rep* 2019;9:5908. DOI PubMed PMC
23. Gao Y, Ota H, Schaler EW, et al. Wearable microfluidic diaphragm pressure sensor for health and tactile touch monitoring. *Adv Mater* 2017;29:1701985. DOI
24. Chang H, Guo R, Sun Z, et al. Direct writing and repairable paper flexible electronics using nickel-liquid metal ink. *Adv Mater*

- Interfaces* 2018;5:1800571. DOI
25. Kim S, Oh J, Jeong D, Bae J. Direct wiring of eutectic gallium-indium to a metal electrode for soft sensor systems. *ACS Appl Mater Interfaces* 2019;11:20557-65. DOI
  26. Yoon Y, Kim S, Kim D, Kauh SK, Lee J. Four degrees-of-freedom direct writing of liquid metal patterns on uneven surfaces. *Adv Mater Technol* 2019;4:1800379. DOI
  27. Guo C, Yu Y, Liu J. Rapidly patterning conductive components on skin substrates as physiological testing devices via liquid metal spraying and pre-designed mask. *J Mater Chem B* 2014;2:5739-45. DOI
  28. Plevachuk Y, Sklyarchuk V, Shevchenko N, Eckert S. Electrophysical and structure-sensitive properties of liquid Ga-In alloys. *Int J Mater Res* 2015;106:66-71. DOI
  29. Plevachuk Y, Sklyarchuk V, Eckert S, Gerbeth G, Novakovic R. Thermophysical properties of the liquid Ga-In-Sn eutectic alloy. *J Chem Eng Data* 2014;59:757-63. DOI
  30. Lu Y, Hu Q, Lin Y, et al. Transformable liquid-metal nanomedicine. *Nat Commun* 2015;6:10066. DOI PubMed PMC
  31. Cicco AD, Filippini A. Local correlations in liquid and supercooled gallium probed by X-ray absorption spectroscopy. *Europhys Lett* 1994;27:407-12. DOI
  32. Tang S, Mitchell DR, Zhao Q, et al. Phase separation in liquid metal nanoparticles. *Matter* 2019;1:192-204. DOI
  33. Koster JN. Directional solidification and melting of eutectic GaIn. *Cryst Res Technol* 1999;34:1129-40. Available from: [https://onlinelibrary.wiley.com/doi/abs/10.1002/\(SICI\)1521-4079\(199911\)34:9%3C1129::AID-CRAT1129%3E3.0.CO;2-P](https://onlinelibrary.wiley.com/doi/abs/10.1002/(SICI)1521-4079(199911)34:9%3C1129::AID-CRAT1129%3E3.0.CO;2-P). [Last accessed on 24 Aug 2023].
  34. Chitambar CR. Medical applications and toxicities of gallium compounds. *Int J Environ Res Public Health* 2010;7:2337-61. DOI PubMed PMC
  35. White SJO, Shine JP. Exposure potential and health impacts of indium and gallium, metals critical to emerging electronics and energy technologies. *Curr Environ Health Rep* 2016;3:459-67. DOI PubMed
  36. Li J, Guo C, Wang Z, Gao K, Shi X, Liu J. Electrical stimulation towards melanoma therapy via liquid metal printed electronics on skin. *Clin Transl Med* 2016;5:21. DOI PubMed PMC
  37. Fan L, Duan M, Xie Z, et al. Injectable and radiopaque liquid metal/calcium alginate hydrogels for endovascular embolization and tumor embolotherapy. *Small* 2019;16:1903421. DOI
  38. Hallfors N, Khan A, Dickey MD, Taylor AM. Integration of pre-aligned liquid metal electrodes for neural stimulation within a user-friendly microfluidic platform. *Lab Chip* 2013;13:522-6. DOI PubMed PMC
  39. Zhang M, Yao S, Rao W, Liu J. Transformable soft liquid metal micro/nanomaterials. *Mate Sci Eng R Rep* 2019;138:1-35. DOI
  40. Domingo JL, Corbella J. A review of the health hazards from gallium exposure. *Trace Elem Med* 1991;8:56-64. Available from: <https://pascal-francis.inist.fr/vibad/index.php?action=getRecordDetail&id=5304637>. [Last accessed on 24 Aug 2023].
  41. Liu S, Sun X, Kemme N, et al. Can liquid metal flow in microchannels made of its own oxide skin? *Microfluid Nanofluid* 2016;20:3. DOI
  42. Regan MJ, Tostmann H, Pershan PS, et al. X-ray study of the oxidation of liquid-gallium surfaces. *Phys Rev B* 1997;55:10786-90. DOI
  43. Cademartiri L, Thuo MM, Nijhuis CA, et al. Electrical resistance of Ag<sup>TS</sup>-S(CH<sub>2</sub>)<sub>n-1</sub>CH<sub>3</sub>//Ga<sub>2</sub>O<sub>3</sub>/EGaIn tunneling junctions. *J Phys Chem C* 2012;116:10848-60. DOI
  44. Dickey MD. Emerging applications of liquid metals featuring surface oxides. *ACS Appl Mater Interfaces* 2014;6:18369-79. DOI PubMed PMC
  45. Zhang Q, Gao Y, Liu J. Atomized spraying of liquid metal droplets on desired substrate surfaces as a generalized way for ubiquitous printed electronics. *Appl Phys A* 2014;116:1091-7. DOI
  46. Gao Y, Li H, Liu J. Direct writing of flexible electronics through room temperature liquid metal ink. *PLoS One* 2012;7:e45485. DOI PubMed PMC
  47. Zheng Y, He ZZ, Yang J, Liu J. Personal electronics printing via tapping mode composite liquid metal ink delivery and adhesion mechanism. *Sci Rep* 2014;4:4588. DOI PubMed PMC
  48. Tang L, Cheng S, Zhang L, et al. Printable metal-polymer conductors for highly stretchable bio-devices. *iScience* 2018;4:302-11. DOI PubMed PMC
  49. Boley JW, White EL, Kramer RK. Mechanically sintered gallium-indium nanoparticles. *Adv Mater* 2015;27:2355-60. DOI PubMed
  50. Ren L, Zhuang J, Casillas G, et al. Nanodroplets for stretchable superconducting circuits. *Adv Funct Mater* 2016;26:8111-8. DOI
  51. Li X, Li M, Zong L, et al. Liquid metal droplets wrapped with polysaccharide microgel as biocompatible aqueous ink for flexible conductive devices. *Adv Funct Mater* 2018;28:1804197. DOI
  52. Li H, Qiao R, Davis TP, Tang SY. Biomedical applications of liquid metal nanoparticles: a critical review. *Biosensors* 2020;10:196. DOI PubMed PMC
  53. Tang S, Qiao R. Liquid metal particles and polymers: a soft-soft system with exciting properties. *Acc Mater Res* 2021;2:966-78. DOI
  54. Lin Y, Cooper C, Wang M, Adams JJ, Genzer J, Dickey MD. Handwritten, soft circuit boards and antennas using liquid metal nanoparticles. *Small* 2015;11:6397-403. DOI PubMed
  55. Liu S, Yuen MC, White EL, et al. Laser sintering of liquid metal nanoparticles for scalable manufacturing of soft and flexible electronics. *ACS Appl Mater Interfaces* 2018;10:28232-41. DOI
  56. Deng B, Cheng GJ. Pulsed laser modulated shock transition from liquid metal nanoparticles to mechanically and thermally robust solid-liquid patterns. *Adv Mater* 2019;31:e1807811. DOI PubMed
  57. Li X, Li M, Xu J, You J, Yang Z, Li C. Evaporation-induced sintering of liquid metal droplets with biological nanofibrils for flexible

- conductivity and responsive actuation. *Nat Commun* 2019;10:3514. DOI PubMed PMC
58. Bartlett MD, Kazem N, Powell-Palm MJ, et al. High thermal conductivity in soft elastomers with elongated liquid metal inclusions. *Proc Natl Acad Sci U S A* 2017;114:2143-8. DOI PubMed PMC
59. Fassler A, Majidi C. Liquid-phase metal inclusions for a conductive polymer composite. *Adv Mater* 2015;27:1928-32. DOI PubMed
60. Markvicka EJ, Bartlett MD, Huang X, Majidi C. An autonomously electrically self-healing liquid metal-elastomer composite for robust soft-matter robotics and electronics. *Nat Mater* 2018;17:618-24. DOI PubMed
61. Ford MJ, Patel DK, Pan C, Bergbreiter S, Majidi C. Controlled assembly of liquid metal inclusions as a general approach for multifunctional composites. *Adv Mater* 2020;32:e2002929. DOI PubMed
62. Tang L, Mou L, Zhang W, Jiang X. Large-scale fabrication of highly elastic conductors on a broad range of surfaces. *ACS Appl Mater Interfaces* 2019;11:7138-47. DOI
63. Wang H, Yao Y, He Z, et al. A highly stretchable liquid metal polymer as reversible transitional insulator and conductor. *Adv Mater* 2019;31:e1901337. DOI
64. Yun G, Tang S, Zhao Q, et al. Liquid metal composites with anisotropic and unconventional piezoconductivity. *Matter* 2020;3:824-41. DOI
65. Yun G, Tang SY, Sun S, et al. Liquid metal-filled magnetorheological elastomer with positive piezoconductivity. *Nat Commun* 2019;10:1300. DOI PubMed PMC
66. Bartlett MD, Fassler A, Kazem N, Markvicka EJ, Mandal P, Majidi C. Liquid metals: stretchable, high-*k* dielectric elastomers through liquid-metal inclusions (Adv. Mater. 19/2016). *Adv Mater* 2016;28:3791. DOI PubMed
67. Kazem N, Bartlett MD, Majidi C. Extreme toughening of soft materials with liquid metal. *Adv Mater* 2018;30:e1706594. DOI PubMed
68. Pan C, Markvicka EJ, Malakooti MH, et al. A liquid-metal-elastomer nanocomposite for stretchable dielectric materials. *Adv Mater* 2019;31:1900663. DOI
69. Kazem N, Hellebrekers T, Majidi C. Soft multifunctional composites and emulsions with liquid metals. *Adv Mater* 2017;29:1605985. DOI PubMed
70. Chen S, Wang H, Zhao R, Rao W, Liu J. Liquid metal composites. *Matter* 2020;2:1446-80. DOI
71. Chen X, Wan H, Guo R, et al. A double-layered liquid metal-based electrochemical sensing system on fabric as a wearable detector for glucose in sweat. *Microsyst Nanoeng* 2022;8:48. DOI PubMed PMC
72. Lin R, Kim HJ, Achavananthadith S, et al. Digitally-embroidered liquid metal electronic textiles for wearable wireless systems. *Nat Commun* 2022;13:2190. DOI PubMed PMC
73. Lee GH, Woo H, Yoon C, et al. A personalized electronic tattoo for healthcare realized by on-the-spot assembly of an intrinsically conductive and durable liquid-metal composite (Adv. Mater. 32/2022). *Adv Mater* 2022;34:2270236. DOI
74. Yang Y, Han J, Huang J, et al. Stretchable energy-harvesting tactile interactive interface with liquid-metal-nanoparticle-based electrodes. *Adv Funct Mater* 2020;30:1909652. DOI
75. Port A, Luechinger R, Albisetti L, et al. Detector clothes for MRI: a wearable array receiver based on liquid metal in elastic tubes. *Sci Rep* 2020;10:8844. DOI PubMed PMC
76. Gu L, Poddar S, Lin Y, et al. A biomimetic eye with a hemispherical perovskite nanowire array retina. *Nature* 2020;581:278-82. DOI
77. Khondoker MAH, Ostashek A, Sameoto D. Direct 3D printing of stretchable circuits via liquid metal co-extrusion within thermoplastic filaments. *Adv Eng Mater* 2019;21:1900060. DOI
78. Teng L, Ye S, Handschuh-wang S, Zhou X, Gan T, Zhou X. Liquid metal-based transient circuits for flexible and recyclable electronics. *Adv Funct Mater* 2019;29:1808739. DOI
79. Chen Y, Liu Y, Ren J, et al. Conformable core-shell fiber tactile sensor by continuous tubular deposition modeling with water-based sacrificial coaxial writing. *Mater Des* 2020;190:108567. DOI
80. Guo R, Tang J, Dong S, et al. One-step liquid metal transfer printing: toward fabrication of flexible electronics on wide range of substrates. *Adv Mater Technol* 2018;3:1800265. DOI
81. Park TH, Kim J, Seo S. Facile and rapid method for fabricating liquid metal electrodes with highly precise patterns via one-step coating. *Adv Funct Mater* 2020;30:2003694. DOI
82. Kim MG, Brown DK, Brand O. Nanofabrication for all-soft and high-density electronic devices based on liquid metal. *Nat Commun* 2020;11:1002. DOI PubMed PMC
83. Abbasi R, Mayyas M, Ghasemian MB, et al. Photolithography-enabled direct patterning of liquid metals. *J Mater Chem C* 2020;8:7805-11. DOI
84. Ozutemiz KB, Wissman J, Ozdoganlar OB, Majidi C. EGaIn-metal interfacing for liquid metal circuitry and microelectronics integration. *Adv Mater Interfaces* 2018;5:1701596. DOI
85. Xu J, Guo H, Ding H, et al. Printable and recyclable conductive ink based on a liquid metal with excellent surface wettability for flexible electronics. *ACS Appl Mater Interfaces* 2021;13:7443-52. DOI
86. Silva CA, Iv J, Yin L, et al. Liquid metal based island-bridge architectures for all printed stretchable electrochemical devices. *Adv Funct Mater* 2020;30:2002041. DOI
87. Zhou L, Fu J, Gao Q, Zhao P, He Y. All-printed flexible and stretchable electronics with pressing or freezing activatable liquid-metal-silicone inks. *Adv Funct Mater* 2020;30:1906683. DOI
88. Guo R, Wang H, Sun X, et al. Semiliquid metal enabled highly conductive wearable electronics for smart fabrics. *ACS Appl Mater*

- Interfaces* 2019;11:30019-27. DOI
89. Guo R, Cui B, Zhao X, et al. Cu-EGaIn enabled stretchable e-skin for interactive electronics and CT assistant localization. *Mater Horiz* 2020;7:1845-53. DOI
  90. Wang J, Cai G, Li S, Gao D, Xiong J, Lee PS. Printable superelastic conductors with extreme stretchability and robust cycling endurance enabled by liquid-metal particles. *Adv Mater* 2018;30:e1706157. DOI PubMed
  91. Guo R, Wang X, Chang H, et al. Ni-GaIn amalgams enabled rapid and customizable fabrication of wearable and wireless healthcare electronics. *Adv Eng Mater* 2018;20:1800054. DOI
  92. Dong C, Leber A, Das Gupta T, et al. High-efficiency super-elastic liquid metal based triboelectric fibers and textiles. *Nat Commun* 2020;11:3537. DOI PubMed PMC
  93. Zhang X, Ai J, Zou R, Su B. Compressible and stretchable magnetoelectric sensors based on liquid metals for highly sensitive, self-powered respiratory monitoring. *ACS Appl Mater Interfaces* 2021;13:15727-37. DOI
  94. Feng B, Jiang X, Zou G, et al. Nacre-inspired, liquid metal-based ultrasensitive electronic skin by spatially regulated cracking strategy. *Adv Funct Mater* 2021;31:2102359. DOI
  95. Mengüç Y, Park Y, Pei H, et al. Wearable soft sensing suit for human gait measurement. *Int J Rob Res* 2014;33:1748-64. DOI
  96. Do TN, Phan H, Nguyen T, Visell Y. Miniature soft electromagnetic actuators for robotic applications. *Adv Funct Mater* 2018;28:1800244. DOI
  97. Xu C, Ma B, Yuan S, Zhao C, Liu H. High-resolution patterning of liquid metal on hydrogel for flexible, stretchable, and self-healing electronics. *Adv Electron Mater* 2020;6:1900721. DOI
  98. Wissman JP, Sampath K, Freeman SE, Rohde CA. Capacitive bio-inspired flow sensing cupula. *Sensors* 2019;19:2639. DOI PubMed PMC
  99. Zhang L, Gao M, Wang R, Deng Z, Gui L. Stretchable pressure sensor with leakage-free liquid-metal electrodes. *Sensors* 2019;19:1316. DOI PubMed PMC
  100. Won D, Baek S, Kim H, Kim J. Arrayed-type touch sensor using micro liquid metal droplets with large dynamic range and high sensitivity. *Sens Actuator A Phys* 2015;235:151-7. DOI
  101. Won D, Baek S, Huh M, Kim H, Lee S, Kim J. Robust capacitive touch sensor using liquid metal droplets with large dynamic range. *Sens Actuator A Phys* 2017;259:105-11. DOI
  102. Yeo JC, Kenry, Yu J, Loh KP, Wang Z, Lim CT. Triple-state liquid-based microfluidic tactile sensor with high flexibility, durability, and sensitivity. *ACS Sens* 2016;1:543-51. DOI
  103. Kim K, Choi J, Jeong Y, et al. Wearable sensors: highly sensitive and wearable liquid metal-based pressure sensor for health monitoring applications: integration of a 3D-printed microbump array with the microchannel. *Adv Healthc Mater* 2019;8:1900986. DOI
  104. Yeo JC, Yu J, Koh ZM, Wang Z, Lim CT. Wearable tactile sensor based on flexible microfluidics. *Lab Chip* 2016;16:3244-50. DOI PubMed
  105. Jeong YR, Kim J, Xie Z, et al. A skin-attachable, stretchable integrated system based on liquid GaInSn for wireless human motion monitoring with multi-site sensing capabilities. *NPG Asia Mater* 2017;9:e443. DOI
  106. Park Y, Majidi C, Kramer R, Bérard P, Wood RJ. Hyperelastic pressure sensing with a liquid-embedded elastomer. *J Micromech Microeng* 2010;20:125029. DOI
  107. Zhang M, Wang X, Huang Z, Rao W. Liquid metal based flexible and implantable biosensors. *Biosensors* 2020;10:170. DOI PubMed PMC
  108. Tepáyotl-ramírez D, Lu T, Park Y, Majidi C. Collapse of triangular channels in a soft elastomer. *Appl Phys Lett* 2013;102:044102. DOI
  109. Nan K, Babae S, Chan WW, et al. Low-cost gastrointestinal manometry via silicone-liquid-metal pressure transducers resembling a quipu. *Nat Biomed Eng* 2022;6:1092-104. DOI PubMed
  110. Zhu M, Wang Y, Lou M, Yu J, Li Z, Ding B. Bioinspired transparent and antibacterial electronic skin for sensitive tactile sensing. *Nano Energy* 2021;81:105669. DOI
  111. Lin X, Mao Y, Li P, et al. Ultra-conformable ionic skin with multi-modal sensing, broad-spectrum antimicrobial and regenerative capabilities for smart and expedited wound care. *Adv Sci* 2021;8:2004627. DOI PubMed PMC
  112. Jiang C, Gao K, Zhao N, et al. A wearable braille recognition system based on high density tactile sensors. In: 2020 IEEE 33rd International Conference on Micro Electro Mechanical Systems (MEMS); 2020 Jan 18-22; Vancouver, Canada; IEEE; 2020. p. 28-31. DOI
  113. Leber A, Dong C, Chandran R, Das Gupta T, Bartolomei N, Sorin F. Soft and stretchable liquid metal transmission lines as distributed probes of multimodal deformations. *Nat Electron* 2020;3:316-26. DOI
  114. Kim S, Oh J, Jeong D, Park W, Bae J. Consistent and reproducible direct ink writing of eutectic gallium-indium for high-quality soft sensors. *Soft Robot* 2018;5:601-12. DOI
  115. Wu Y, Zhen R, Liu H, et al. Liquid metal fiber composed of a tubular channel as a high-performance strain sensor. *J Mater Chem C* 2017;5:12483-91. DOI
  116. Lu T, Wissman J, Ruthika, Majidi C. Soft anisotropic conductors as electric vias for Ga-based liquid metal circuits. *ACS Appl Mater Interfaces* 2015;7:26923-9. DOI PubMed
  117. So J, Thelen J, Qusba A, Hayes GJ, Lazzi G, Dickey MD. Reversibly deformable and mechanically tunable fluidic antennas. *Adv*

- Funct Mater* 2009;19:3632-7. DOI
118. Tang L, Shang J, Jiang X. Multilayered electronic transfer tattoo that can enable the crease amplification effect. *Sci Adv* 2021;7:eabe3778. DOI PubMed PMC
  119. Kramer RK, Majidi C, Sahai R, Wood RJ. Soft curvature sensors for joint angle proprioception. In: 2011 IEEE/RSJ International Conference on Intelligent Robots and Systems; 2011 Sep 25-30; San Francisco, CA, USA. IEEE; 2011. DOI
  120. Li G, Zhang M, Liu S, et al. Three-dimensional flexible electronics using solidified liquid metal with regulated plasticity. *Nat Electron* 2023;6:154-63. DOI
  121. Uchida K, Takahashi S, Harii K, et al. Observation of the spin Seebeck effect. *Nature* 2008;455:778-81. DOI
  122. Adachi H, Uchida K, Saitoh E, Maekawa S. Theory of the spin Seebeck effect. *Rep Prog Phys* 2013;76:036501. DOI PubMed
  123. Li H, Yang Y, Liu J. Printable tiny thermocouple by liquid metal gallium and its matching metal. *Appl Phys Lett* 2012;101:073511. DOI
  124. Wang Q, Gao M, Zhang L, Deng Z, Gui L. A handy flexible micro-thermocouple using low-melting-point metal alloys. *Sensors* 2019;19:314. DOI PubMed PMC
  125. Yu Y, Zhang J, Liu J. Biomedical implementation of liquid metal ink as drawable ECG electrode and skin circuit. *PLoS One* 2013;8:e58771. DOI PubMed PMC
  126. Guo R, Sun X, Yao S, et al. Semi-liquid-metal-(Ni-EGaIn)-based ultraconformable electronic tattoo. *Adv Mater Technol* 2019;4:1900183. DOI
  127. Timosina V, Cole T, Lu H, et al. A non-newtonian liquid metal enabled enhanced electrography. *Biosens Bioelectron* 2023;235:115414. DOI
  128. Ding L, Hang C, Cheng S, et al. A soft, conductive external stent inhibits intimal hyperplasia in vein grafts by electroporation and mechanical restriction. *ACS Nano* 2020;14:16770-80. DOI
  129. Cheng S, Hang C, Ding L, et al. Electronic blood vessel. *Matter* 2020;3:1664-84. DOI
  130. Liu F, Yu Y, Yi L, Liu J. Liquid metal as reconnection agent for peripheral nerve injury. *Science Bulletin* 2016;61:939-47. DOI
  131. Dong R, Wang L, Hang C, et al. Printed stretchable liquid metal electrode arrays for in vivo neural recording. *Small* 2021;17:e2006612. DOI
  132. Wen X, Wang B, Huang S, et al. Flexible, multifunctional neural probe with liquid metal enabled, ultra-large tunable stiffness for deep-brain chemical sensing and agent delivery. *Biosens Bioelectron* 2019;131:37-45. DOI PubMed PMC
  133. Lim T, Kim M, Akbarian A, Kim J, Tresco PA, Zhang H. Conductive polymer enabled biostable liquid metal electrodes for bioelectronic applications. *Adv Healthc Mater* 2022;11:e2102382. DOI PubMed
  134. Wang S, Nie Y, Zhu H, et al. Intrinsically stretchable electronics with ultrahigh deformability to monitor dynamically moving organs. *Sci Adv* 2022;8:eabl5511. DOI PubMed PMC
  135. Li G, Ma X, Xu Z, et al. A crack compensation strategy for highly stretchable conductors based on liquid metal inclusions. *iScience* 2022;25:105495. DOI PubMed PMC
  136. Schedle A, Samorapoompichit P, Rausch-Fan XH, et al. Response of L-929 fibroblasts, human gingival fibroblasts, and human tissue mast cells to various metal cations. *J Dent Res* 1995;74:1513-20. DOI
  137. Kim JH, Kim S, So JH, Kim K, Koo HJ. Cytotoxicity of gallium-indium liquid metal in an aqueous environment. *ACS Appl Mater Interfaces* 2018;10:17448-54. DOI
  138. Zhang C, Yang B, Biazik JM, et al. Gallium nanodroplets are anti-inflammatory without interfering with iron homeostasis. *ACS Nano* 2022;16:8891-903. DOI